Desalination and Water Treatment
www.deswater.com

46 (2012) 139–148
August

1944-3994/1944-3986 © 2012 Desalination Publications. All rights reserved
doi: 10.1080/19443994.2012.677495

Taylor & Francis
Taylor & Francis Group

Removal of humic substances with different apparent molecular sizes using Fenton's reagent

Marcelo De Julio[a,*], Luiz Di Bernardo[b], Tatiane Sakamoto De Julio[c], Sandro Xavier de Campos[d], Eny Maria Vieira[e]

[a]*Civil Engineering Division, Aeronautic Institute of Technology (ITA), Praça Marechal Eduardo Gomes, n° 50, Vila das Acácias, São José dos Campos, SP 12.228-900, Brazil*
Tel. +55 12 3947 6805; Fax: +55 12 3947 6801; email: dejulio@ita.br
[b]*Department of Hydraulics and Sanitation, São Carlos School of Engineering, University of São Paulo (EESC-USP), Av. Trabalhador Sãocarlense, n°400, Centro, São Carlos, SP 13.566-590, Brazil*
[c]*Department of Civil Engineering, University of Taubaté (UNITAU), Rua Exped. Ernesto Pereira, n° 99, Centro, Taubaté, SP 12.020-330, Brazil*
[d]*Department of Chemistry, Ponta Grossa State University (UEPG), Av. Carlos Cavalcanti, n° 4748, Campus Uvaranas, Ponta Grossa, PR 84.030-900, Brazil*
[e]*São Carlos Chemistry Institute, University of São Paulo (IQSC-USP), Av. Trabalhador Sãocarlense, n° 400, Centro, São Carlos, SP 13.566-590, Brazil*

Received 8 August 2011; Accepted 20 February 2012

ABSTRACT

Fenton's reagent was used as a coagulating agent in the treatment of water samples with high true color caused by humic substances (HS) extracted from peat. The effects of the apparent molecular size of HS on coagulation, flocculation, and flotation were studied. Four distinct water samples having the same true colors were prepared using HS with different molecular sizes obtained through ultrafiltration fractioning. Through optimization of the coagulant dosage and coagulation pH and the construction of coagulation diagrams for each water sample, it was verified that the sample with the smallest apparent molecular size of HS was the most difficult to treat, requiring higher coagulant (Fenton's reagent) dosages than samples prepared with larger HS molecular sizes. Furthermore, filtration experiments after dissolved air flotation were carried out to simulate conventional treatment. The most representative results in filtered water were: absorbance at 254 nm $\leqslant 0.016\,\text{cm}^{-1}$; apparent color $\leqslant 3$ HU; and residual iron concentration $< 0.005\,\text{mg L}^{-1}$. The total organic carbon values of filtered water samples were also very low, always $< 1.0\,\text{mg L}^{-1}$.

Keywords: Coagulation; DAF; Drinking water; Fenton's reagent; Humic substances; Molecular size

1. Introduction

Humic substances (HS) are a heterogeneous mixture of dark-colored organic macromolecules of complex composition; they are present in soil and aquatic ecosystems and function as effective carbon reservoirs that prevent carbon dioxide emission. HS comprise 60–70% of the total carbon in soil and 60–90% of the dissolved carbon in natural water [1]. HS are not well defined, but can generally be subdivided into three fractions: humins, which represent the insoluble humic components of aqueous solutions

---

*Corresponding author.

at all pH values; humic acids (HAs), which are soluble in alkaline and weakly acidic solutions, but precipitate at or below pH 2.0; and fulvic acids (FAs), which are soluble in aqueous solutions at all pH values [2]. Humic materials may be specifically targeted for the removal from potable water supplies because they can adversely affect the appearance and taste and they can react with chlorine to form potentially carcinogenic chlorinated organic compounds [3,4]. Furthermore, the presence of dissolved organic matter may reduce the effectiveness of water treatment processes that employ membranes or microporous adsorbents [5,6]. Even when not specifically targeted for removal, macromolecular dissolved organic matter has been shown to compete with low molecular weight synthetic organic chemicals, reducing their adsorption rates and equilibrium capacities [7–10]. The removal of (or the reduction in concentration of) such organic matter is therefore an important factor in water treatment.

The flocs formed by HS coagulation are relatively small and have low specific masses [11], mainly with low turbidity and high true color. As a result, their removal by sedimentation is limited. Thus, the use of dissolved air flotation (DAF) is an interesting technology for the clarification of water with these characteristics.

The use of Fenton's reagent, which entails adding Fe^{+2} ions and hydrogen peroxide (H_2O_2) under acidic conditions, is advantageous for drinking water treatment because it provides both pre-oxidation and coagulation in a single process. As shown in Eq. (1), Fenton's reaction forms the hydroxyl free radical ($OH^\bullet$), which is a highly reactive and nonselective intermediate oxidant capable of effectively oxidizing numerous organic substances [12,13]. Because both Fe^{+2} and Fe^{+3} ions form hydrolyzed species that act as coagulants, Fenton's reagent can have the dual function of oxidation and coagulation during treatment processes.

$$Fe^{+2} + H_2O_2 \rightarrow Fe^{+3} + OH^\bullet + OH^- \tag{1}$$

The strong oxidative power of Fenton's reagent that results from the hydroxyl radical ($OH^\bullet$) is also advantageous because pre-oxidation is becoming increasingly necessary to address poor raw water quality. With Fenton's reagent, undesirable halogenated by-products are not formed (since no chlorine or halogenated disinfectants were used). Fenton's reagent is further advantageous for natural organic matter (NOM) removal because the coagulants traditionally used in water treatment (aluminum or iron salts) are frequently incapable of removing recalcitrant NOM [14], making alternative treatment processes necessary. Advanced oxidative processes (AOP), including the application of Fenton's reagent, have thus been introduced as alternatives.

There is a dearth of reports on the degradation of HS using Fenton's reagent [8,15–17]. Some studies have shown the influence of the apparent molecular sizes of HS on coagulation with traditional coagulants, flocculation, and sedimentation [18,19], but data on the use of DAF and Fenton's reagent to treat water with high true color are limited.

Thus, the main objective of this study was to evaluate the absorbance removal efficiency from water samples containing HS with different apparent molecular sizes, but with the same true color. For this, coagulation, flocculation and flotation tests were performed using Fenton coagulation to determine the most suitable pH ranges and the dosages of Fe^{+2} in the Fenton process and then how to improve the following coagulation efficiency.

2. Materials and methods

2.1. Collection and extraction of HS

HS were extracted from peat soil collected from the banks of the Mogi Guaçu River in Brazil (latitude 21.5° S and longitude 47.9° W). Peat samples were dried and then coarsely ground in an agate mortar. The HS extraction method was as follows: the peat was added to a KOH extraction solution ($0.5\,mol\,L^{-1}$) in a 1:20 (m/v) ratio; this solution was mixed for 4 h at room temperature (~25 °C) and then allowed to sediment for 48 h, after which the supernatant was stored in semi-permeable paper bags. These bags were placed in a hydrochloric acid solution (HCl 1%) until the HS extracts reached a pH close to 6.0. Finally, residual Cl^- was removed via dialysis in non-chlorinated water until HS samples tested negative for chloride (using an $AgNO_3$-based test).

Following extraction, the HS solution was frozen and stored in plastic bottles.

2.2. Ultrafiltration (UF) fractionation of HS

The extracted HS were diluted to a concentration of $1.0\,mg\,mL^{-1}$ using groundwater. The solution was vacuum filtered using a 0.45 μm (Millipore) membrane for subsequent UF fractionation (*polyethersulfone* membranes, Vivaflow 50, Sartorius group, tangential flow, Vivascience). During HS fractionation, a sample concentration method using recirculation was adopted [20]. The maximum applied flow rate was $300\,mL\,min^{-1}$ with 1.5 bar pressure. The following apparent molecular size fractions were obtained: between 100 kDa and 0.45 μm; between 30 and 100 kDa; and <30 kDa. A composite sample containing all size fractions was also obtained, which was only filtered through the 0.45 μm membrane.

2.3. Water samples

Four distinct water samples were prepared for each of the three HS size fractions (100 kDa–0.45 μm, 30–100 kDa and <30 kDa) and the composite fraction (0.45 μm filtered). Each HS fraction was added separately to groundwater. The four water samples exhibited true color values of 100 ± 5 HU (Hazen units), and the pH of each sample was adjusted to 5.0 ± 0.1.

2.4. Coagulation, flocculation, and flotation tests

Coagulation diagrams were built for the four water samples by varying the coagulant dosage (Fenton's reagent) and the coagulation pH; 0.1 M sodium hydroxide (NaOH; AR Mallinckrodt) and hydrochloric acid (HCl; 36.5–38%, P.A., Synth) solutions were used to vary the coagulation pH. The temperature of the water samples was maintained at 20 ± 1 ℃.

Ferrous sulfate (P.A.—ACS, J.T. Baker) and a 0.1 M solution of hydrogen peroxide (29%, P.A.—ACS, Synthy) were applied as Fenton's reagent. A stock solution of ferrous sulfate was prepared at a concentration of $10\,\mathrm{g\,L^{-1}}$.

Fenton's reagent was applied as a coagulant as follows: first, $FeSO_4{\cdot}7H_2O$ was added, followed by H_2O_2. Immediately after the addition of these chemical products, a sample was collected for oxidation pH measurement (this pH value was a little lower than the water sample pH—see Table 1—because of the addition of ferrous sulfate); 1.5 min was allowed for oxidation time (the average velocity gradient of this step was the same as for the rapid-mix step). After this time, the alkalinizing or acidifying agent was added (marking the start of rapid-mix time) and another sample was collected for coagulation pH measurement. The hydrogen peroxide dosage was equal to three times (3×) the stoichiometric dosage required for Fenton's reagent (Eq. (1)); this ratio was employed for all tested ferrous sulfate dosages. For example, the mass of 1 mol of $FeSO_4{\cdot}7H_2O$ is 278.02 g, which corresponds to a Fe^{+2} mass of 55.85 g. According to Eq. (1), 1 mol of Fe^{+2} reacts with 1 mol of H_2O_2 (with a weight ratio of 34.01/55.85). Thus, a $FeSO_4{\cdot}7H_2O$ dosage of $15\,\mathrm{mg\,L^{-1}}$ corresponds to $3.01\,\mathrm{mg\,L^{-1}}$ of Fe^{+2} ($15 \times 55.85/278.02$); 1:1 stoichiometry calls for a H_2O_2 dosage of $1.83\,\mathrm{mg\,L^{-1}}$ ($3.01 \times 34.01/55.85$). For a 3× dosage, $5.5\,\mathrm{mg\,L^{-1}}$ of H_2O_2 (3×1.83) is required.

All experiments were performed in flotest equipment (Nova Ética, Brazil) using three square 2 L flasks under the following conditions: rapid mix (time, $T_{rm} = 10\,\mathrm{s}$; velocity gradient, $G_{rm} = 1{,}000\,\mathrm{s^{-1}}$); flocculation ($T_{fl} = 15\,\mathrm{min}$; $G_{fl} = 25\,\mathrm{s^{-1}}$); and DAF (saturation chamber pressure = 400 kPa; saturation time = 8 min; recirculation rate = 15%; flotation velocities (V_f) of 15, 10, and $5\,\mathrm{cm\,min^{-1}}$). The measured parameters during these experiments were oxidation pH, coagulation pH (Digimed), remaining UV_{254} absorbance ($\mathrm{cm^{-1}}$; subnatant), and remaining apparent color (DR/4,000 U, Hach, spectrophotometer). During all pH measurements, samples were stirred using a magnetic stirrer (Quimis). In all absorbance and color measurements, the dilution caused by the introduction of saturated water was taken into account.

For each water sample, a pair of 'coagulant dosage versus coagulation pH´ values was selected in the respective diagrams based on remaining UV_{254} absorbance and apparent color removal and taking into account the three flotation velocities studied. Although twenty-four coagulation diagrams were generated, only the diagrams for UV_{254} absorbance and $V_f = 5\,\mathrm{cm\,min^{-1}}$ are presented.

In the coagulation diagrams, the absorbance is reported as the percentage $[(A/A_0) \times 100]$, where A is the remaining UV_{254} absorbance ($\mathrm{cm^{-1}}$) and A_0 is the UV_{254} absorbance ($\mathrm{cm^{-1}}$) of the water sample. The abbreviation CI indicates that coagulation was inefficient. Floc formation was not observed for these points and, consequently, absorbance and color were not measured.

2.5. Coagulation, flocculation, flotation, and filtration tests

With the selected pair of 'coagulant dosage versus coagulation pH' values for each water sample, two coagulation, flocculation, flotation, and filtration tests were carried out to simulate a conventional treatment process. The following parameters were measured in filtered water: UV_{254} absorbance; apparent color; turbidity (2100P, Hach, Turbidimeter); total organic carbon (TOC analyzer 5,000A, Shimadzu); and total iron concentration (atomic absorption spectrophotometer, model AA-1,275, Varian).

The filtration step employed a filter column coupled immediately downstream from the flotest flask. The filter column was a 19-mm internal diameter acrylic tube containing sand as the filter media (10 cm deep) with a granulometric range between 0.59 and 1.41 mm. The average filtration flow rate was $16\,\mathrm{mL\,min^{-1}}$ (corresponding to a filtration rate of $80\,\mathrm{m^3\,(m^2\,d)^{-1}}$), and samples of the filtered water

Table 1
Results for sand filtration tests after DAF for the four water samples

pH_{oxid}	pH_{coag}	pH_{flot}	pH_{filtr}	Rem. ap. col. after flotation (HU)*	254 nm rem. Abs** after flotation (cm^{-1})*	% rem. Abs after flotation - $(A/A_0) * 100$	Rem. ap. col. after filtration (HU)	254 nm Abs after filtration (cm^{-1})	% rem. Abs after filtration - $(A/A_0) * 100$	Turbidity after filtration (NTU)	TOC after filtration (mg L^{-1})
Water sample 1											
4.31	5.87	6.41	6.50	34	0.060	39	1	0.007	5	0.40	0.376
4.34	5.81	6.35	6.52	37	0.065	43	1	0.011	7	0.29	0.398
Water sample 2											
4.72	6.02	6.34	6.55	37	0.046	33	<1	0.007	5	0.30	0.329
4.67	5.98	6.27	6.55	41	0.049	36	<1	0.008	6	0.33	0.393
Water sample 3											
3.80	5.60	5.85	5.94	32	0.046	29	3	0.004	3	0.44	0.586
3.80	5.66	5.93	6.16	36	0.054	34	3	0.006	3	0.41	0.533
Water sample 4											
3.70	5.89	6.08	6.08	49	0.078	29	3	0.016	6	0.48	0.915
3.65	5.70	5.86	5.91	49	0.082	30	3	0.016	6	0.55	0.850

Notes: Water samples characterization can be seen in Figs. 1– 4.

*Flotation velocity = 5 cm min^{-1}.

**Abs: 254 nm absorbance (cm^{-1}).

Water sample 1—HS fraction filtered through a 0.45 μm membrane with 15 mg L^{-1} of $FeSO_4{\cdot}7H_2O$; 5.5 mg L^{-1} of H_2O_2; and 4.5 mg L^{-1} of NaOH.

Water sample 2—HS fraction filtered through a 0.45 μm membrane and >100 kDa with 7.5 mg L^{-1} of $FeSO_4{\cdot}7H_2O$; 2.75 mg L^{-1} of H_2O_2; and 3.0 mg L^{-1} of NaOH.

Water sample 3—HS fraction with apparent molecular size between 30 and 100 kDa with 20 mg L^{-1} of $FeSO_4{\cdot}7H_2O$; 7.3 mg L^{-1} of H_2O_2; and 6.0 mg L^{-1} of NaOH.

Water sample 4—HS fraction with apparent molecular size <30 kDa with 40 mg L^{-1} of $FeSO_4{\cdot}7H_2O$; 14.7 mg L^{-1} of H_2O_2; and 12.0 mg L^{-1} of NaOH.

were collected 30 min after the flotation time (flotation velocity 5 cm min^{-1}). Because the filters were backwashed with tap water, it was necessary to filter for 30 min to flush this water out of the filters before collecting samples.

3. Results and discussion

3.1. Coagulation diagrams

Figs. 1–4 show the coagulation diagrams for the four water samples. Hydrogen peroxide and ferrous sulfate dosages are shown in the left-hand *y*-axes, while the correspondent iron-II dosages are shown in the right. The coagulation pH is plotted as the abscissa. The main characteristics of each water sample are also shown.

According to classical theories, there are two predominant mechanisms of metal ion coagulation: 'charge neutralization' and 'sweep coagulation'; the former occurs at lower pH conditions with the coagulant in the cationic form (e.g. $Fe(OH)^{2+}$, $Fe(OH)_2^+$) and the latter at higher pH and higher doses where the coagulant precipitates as a metal hydroxide [21].

An analysis of Figs. 1–4 reveals two regions in which coagulation with Fenton's reagent and subsequent flocculation and flotation produce removal efficiencies ⩾ 50 and 60% for the first (lower pH) and second (higher pH) regions, respectively. A similar behavior was observed by Edwards and Amirtharajah [22], who also worked with a water sample with a true color of 100 HU (caused by the addition of HA) and a turbidity equal to zero, using aluminum sulfate (alum) as a coagulant. These researchers concluded that in the first region, corresponding to approximate coagulation pH values of 3.6–4.6 in the current study (Figs. 1–4), the hydrolyzing species adsorption mechanism was probably dominant, causing charge neutralization of HS molecules. In the second region, which is approximately between pH 5.6 and 6.6 in the current study, Fe $(OH)_3$ precipitate formation was observed and removal possibly occurred via adsorption of HS molecules and their incorporation into the precipitate. Furthermore, coagulant dosages (Fenton) were lower in the first region than in the second region. As observed by Edwards and Amirtharajah [22], there seems to be a restabilization region between the two regions in which coagulation resulted efficient.

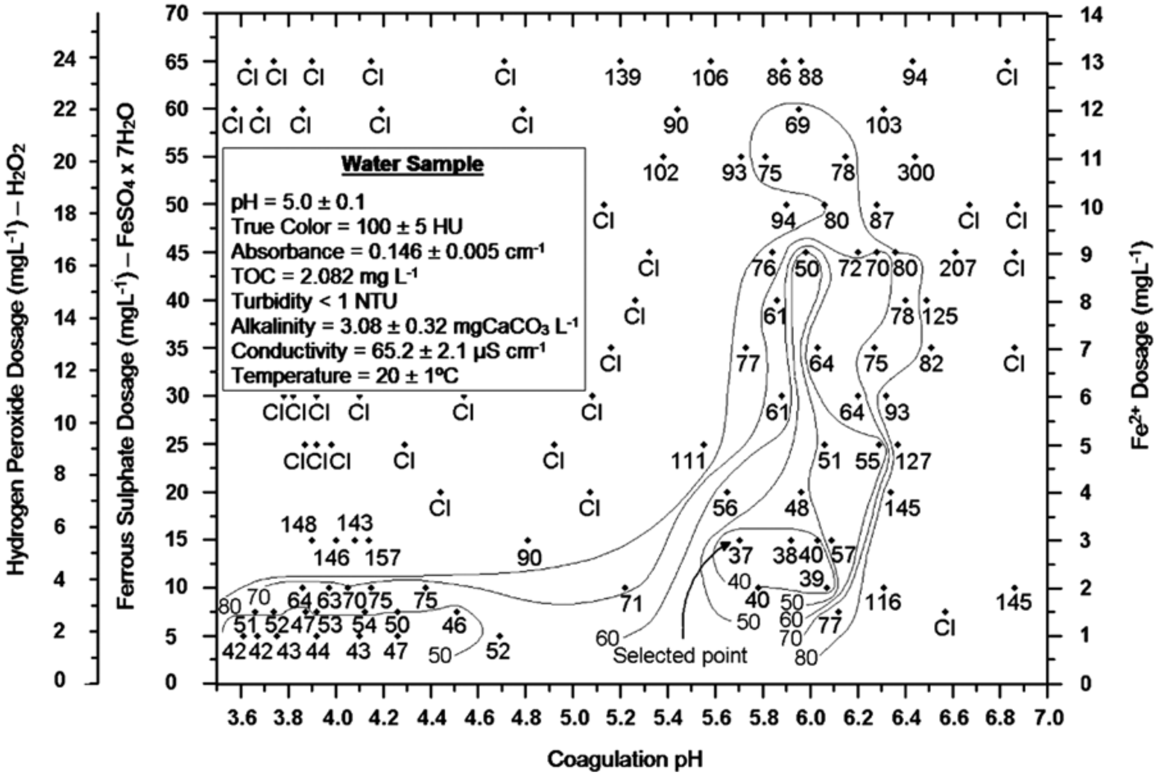

Fig. 1. Fenton dose versus pH coagulation diagram—percentage absorbance at 254 nm remaining [$(A/A_0) \times 100$] for the water sample with the HS fraction filtered through a 0.45 µm membrane ($V_f = 5\,cm\,min^{-1}$). Note: CI indicates that the coagulation was inefficient.

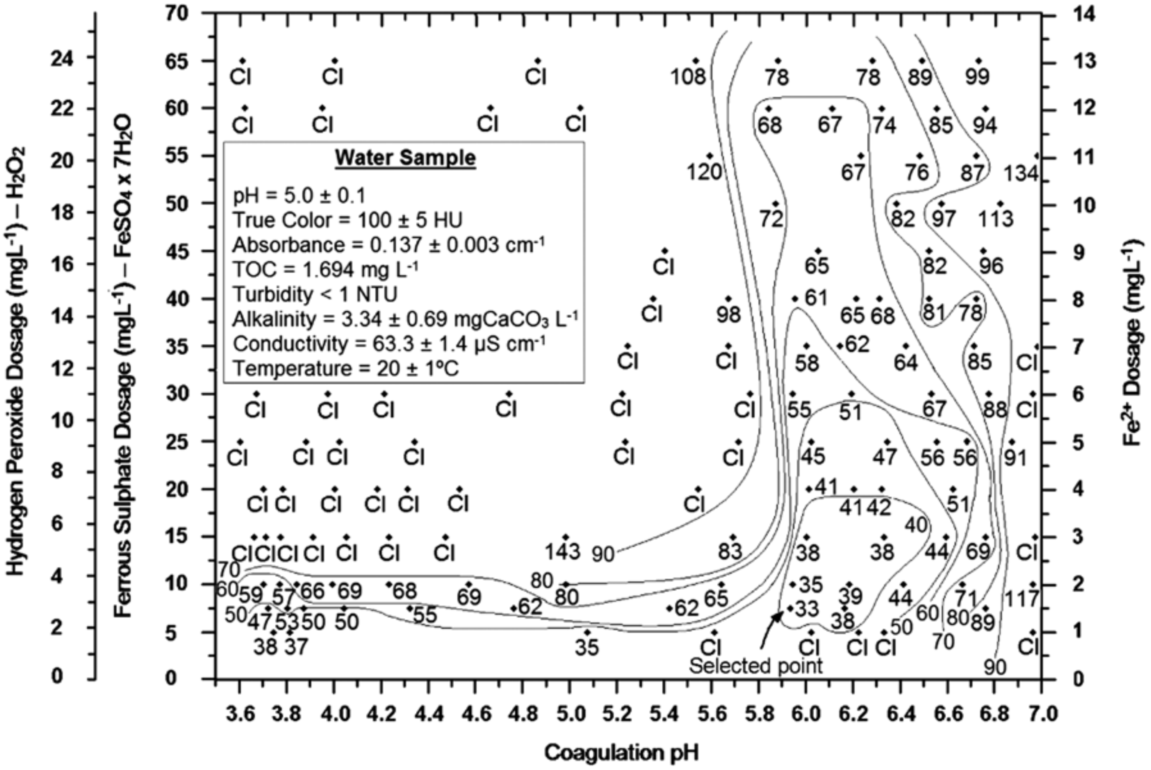

Fig. 2. Fenton dose versus pH coagulation diagram—percentage absorbance at 254 nm remaining $[(A/A_0) \times 100]$ for the water sample with the HS fraction filtered through a 0.45 µm membrane with apparent molecular size >100 kDa ($V_f = 5\,\text{cm min}^{-1}$).

While the Fenton reaction is a combination of oxidation and coagulation, these results suggest that coagulation using Fenton's reagent produces behavior similar to those observed in studies using other coagulants such as ferric chloride and alum. Moreover, oxidation and coagulation probably both remove HS, the former changes the chemical structures of HS molecules and the latter transfers HS from one phase to another. Typically, at a low pH, the removal of hydroxyl radical-induced oxidation is maximized, so that the overall removal (due to oxidation and coagulation) may peak in the first region (low pH side). In contrast, at neutral pH, coagulation efficiency may be maximized, so that the overall removal peaks in the second region.

For the water sample with the HS fraction filtered through a 0.45 µm membrane and with an apparent HS molecular size >100 kDa, it is evident that the regions formed in the coagulation diagram are wider and the isoefficient curves containing the best results (lower percentage absorbance remaining) comprise a larger area in Fig. 2 than in Fig. 1. Furthermore, the highest absorbance removal efficiency was observed at a ferrous sulfate dosage of 7.5 mg L^{-1} for the water sample with an apparent HS molecular size fraction between 100 kDa and 0.45 µm, whereas for the water sample with the HS fraction filtered only through a 0.45 µm membrane, the dosage was between 10 and 15 mg L^{-1} (with similar coagulation pH values). These results can be explained by the hypothesis that for this water sample (between 100 kDa and 0.45 µm), the smallest HS molecules (<100 kDa) were removed. According to Campos et al. [19], these molecules have higher FA than HA concentrations and have higher proportions of bound oxygen groups. These authors concluded that these groups therefore have greater amounts of negative charge due to the non-bonded electrons, which favor repulsion between these electrons and colloidal particles thereby negatively influencing the coagulation process.

Campos et al. [19] worked with the same HS used in the present research and characterized the different fractions using nuclear magnetic resonance (NMR) and infrared spectroscopy (IR) in addition to determining the percentage of HA and FA.

For the water sample with the HS apparent molecular size fraction between 30 and 100 kDa (Fig. 3), the isoefficiency curves leading to the most effective coagulation were shifted to a slightly lower coagulation pH range (for the second region in the diagrams). For

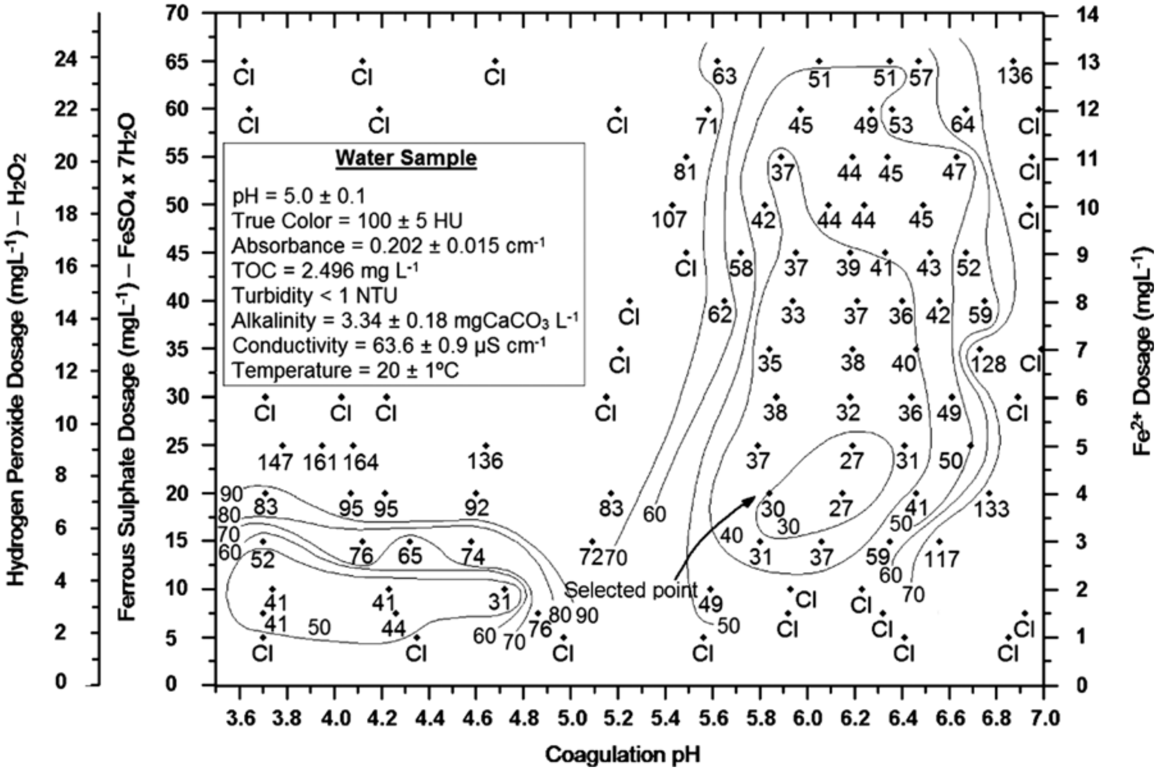

Fig. 3. Fenton dose versus pH coagulation diagram—percentage absorbance at 254 nm remaining [$(A/A_0) \times 100$] for the water sample with the HS fraction with apparent molecular size between 30 and 100 kDa ($V_f = 5\,\text{cm}\,\text{min}^{-1}$).

the size fraction <30 kDa (Fig. 4), these curves showed a more accentuated shift, indicating that the smallest HS molecules, which present higher FA concentrations in relation to HA and higher proportions of bound oxygen groups [19], required a somewhat inferior coagulation pH range in comparison with the larger HS molecules.

For the fraction <30 kDa, ferrous sulfate dosages of up to 15 mg L^{-1} (for the second region on the coagulation diagrams) were required for floc formation, indicating that lower dosages were insufficient to destabilize the HS. However, for the larger apparent HS molecular sizes (Fig. 2), higher removal efficiencies were reached at dosages lower than or equal to this value.

As previously mentioned, the coagulation diagrams were constructed for flotation velocities of 15, 10, and 5 cm min^{-1} and for remaining apparent color and UV_{254} absorbance. All of these factors were taken into account when the selected point (which corresponds to a pair of 'coagulation dosage versus coagulation pH' values) was chosen, and because of this, the lowest percentage absorbance remaining found in the diagrams for $V_f = 5\,\text{cm}\,\text{min}^{-1}$ was not always selected.

A general analysis of all the coagulation diagrams (Figs. 1–4) reveals that the selected point for the HS fraction with an apparent molecular size between 30 and 100 kDa required a coagulant dosage (Fenton; 4.02 mg $\text{Fe}^{+2}\,\text{L}^{-1}$ and 7.34 mg $\text{H}_2\text{O}_2\,\text{L}^{-1}$) close to 166% higher (in relation of Fe^{+2}) than that required for the selected point for the HS fraction between 100 kDa and 0.45 µm (1.51 mg $\text{Fe}^{+2}\,\text{L}^{-1}$ and 2.75 mg $\text{H}_2\text{O}_2\,\text{L}^{-1}$) and close to 33% higher than that required for the water sample having the HS fraction only filtered through a 0.45 µm membrane (3.01 mg $\text{Fe}^{+2}\,\text{L}^{-1}$ and 5.50 mg $\text{H}_2\text{O}_2\,\text{L}^{-1}$). The selected point for the HS fraction <30 kDa (8.04 mg $\text{Fe}^{+2}\,\text{L}^{-1}$ and 14.68 mg $\text{H}_2\text{O}_2\,\text{L}^{-1}$) required twice the dosage needed for the fraction between 30 and 100 kDa, and approximately 432% higher than that for the fraction between 100 kDa and 0.45 µm.

Ratnaweera et al. [18] also fractionated HS (composed of NOM extracted from natural water by reverse osmosis) using UF (employing *polyethersulfone* membranes with tangential flow) in different apparent molecular sizes (<10 kDa, between 10 and 50 kDa, between 50 and 100 kDa, and >100 kDa) and observed that the HS of larger apparent molecular size required lower coagulant dosages in comparison with those of smaller apparent molecular size. These experiments were performed in a jar test apparatus and included coagulation, flocculation, and sedimentation. Campos

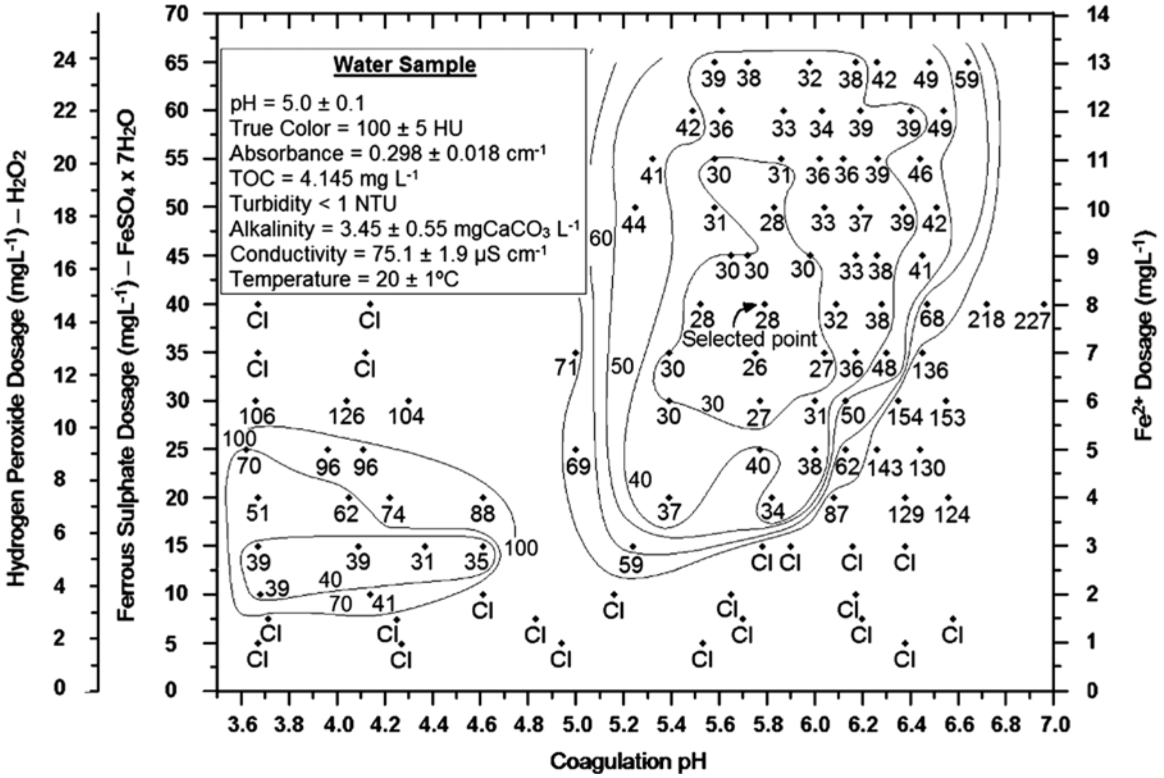

Fig. 4. Fenton dose versus pH coagulation diagram—percentage absorbance at 254 nm remaining [$(A/A_0) \times 100$] for the water sample with the HS fraction with apparent molecular size <30 kDa ($V_f = 5\,\mathrm{cm\,min^{-1}}$).

et al. [19] also performed jar test experiments using coagulation, flocculation, and sedimentation with alum as a coagulant and found similar results. Thus, it is possible to conclude that, regardless of the coagulant used (even Fenton's reagent, which is both an oxidant and a coagulant) and the clarification technology (sedimentation or flotation) employed, waters predominantly containing HS molecules of smaller apparent sizes are more difficult to treat.

As verified by Campos et al. [19], the smallest HS fraction presented a higher percentage of FAs in relation to HAs. The FAs have smaller chains with structures dominated by aliphatics, a higher number of functional carboxylic groups and phenolic and alcoholic hydroxyls. These characteristics make the HS more hydrophilic and acidic [2]. These findings suggest that not only the apparent molecular size but also the structural characteristics of HS fractions play a significant role in the coagulation process.

3.2. Filtration experiments after DAF

Table 1 shows the results of filtration experiments following DAF (two replicate experiments for each water sample). The chemical product dosages applied correspond to the dosages of the selected points on the coagulation diagrams (Figs. 1–4) for each water sample.

An analysis of Table 1 shows that the remaining apparent colors and turbidities after filtration were always ⩽ 3 HU and 0.50 NTU (except for the last experiment, in which this value was ⩽0.55), respectively. Total iron concentrations after filtration were <0.005 mg L^{-1} (below the detection limit for all samples). The new Brazilian drinking water standard [23] set a maximum value for apparent color after filtration of 15 HU (the same value recommended by the WHO [24] and the US-EPA [25]) and a maximum turbidity value of 1 NTU after rapid filtration (the same value required by the Council Directive [26] for the treatment of superficial waters), and established that the turbidity must be ⩽ 5 NTU in at least 95% of the samples taken in any month (having a four-year period to achieve this, since the new Brazilian standard was published in December 2011). The US drinking water standards [25] establish that, for systems that use conventional or direct filtration, at no time should turbidity go higher than 1 NTU and the turbidity must be ⩽ 0.3 NTU in at least 95% of the samples taken in any month. The maximum total iron concentrations for Brazilian [23] and US [25], and European [26] drinking water standards are 0.3 and 0.2 mg L^{-1}, respectively. Thus, the coagulation, flocculation, DAF and the filtration treatment employing Fenton's reagent as coagulant meets Brazilian and European drinking water standards (in relation to the measured parameters) for the four water samples studied. In relation to US standards, only the turbidity standard was not met; this could be accomplished in a real treatment plant by optimization of the filtration process (with the use of a deeper filter).

Water samples prepared with the smallest apparent HS molecular sizes also had higher TOC concentrations in the filtered water compared to water prepared with larger apparent HS molecular sizes (Table 1), indicating that the smallest HS size fractions were more difficult to remove (however, it should be noticed that the initial TOC of Water sample 4 was also the highest—4.145 mg/L). An et al. [27] verified that coagulation, flocculation, sedimentation, and sand filtration were more efficient at removing the larger molecular size fractions. This supports the results found in coagulation diagrams. Even with a membrane process [28], the smallest HA molecules were more difficult to remove and a pre-treatment step with coagulation/flocculation with ferric chloride was necessary to improve the removal (up to 90%).

According to Edzwald [29] and Selcuk et al. [4], disinfection by-product (DBP) concentrations depend on several factors, predominant among which are TOC, UV_{254}, disinfectant type, and disinfectant concentration. One way to minimize the by-product formation is to limit the TOC concentration of filtered water. To adequately reduce the risk of DBP formation, according to Singer [30], TOC concentrations (in filtered water) must be $<2.0\,\mathrm{mg\,L^{-1}}$. In this work, TOC concentrations were well below safe levels (always $<1.0\,\mathrm{mg\,L^{-1}}$), with an average removal efficiency for all HS fractions of 80%. Then, this treatment is capable of reducing the DBPs in treated water (Brazilian standards also require that water be disinfected with chlorine and an adequate residual be maintained).

The results of this study suggest that the application of Fenton's reagent in water treatment plants (WTP) may be beneficial because this product does not contribute to the formation of halogenated pre-oxidation by-products. In addition, Fenton's reagent accomplishes both pre-oxidation and coagulation, and as observed, conventional treatment (coagulation, flocculation, DAF, and filtration) using Fenton's reagent as a coagulant results in lower TOC and UV_{254} absorbance values for the filtered water produced. Therefore, Fenton's reagent seems to be a promising alternative for the treatment of waters containing high concentrations of organic compounds.

4. Conclusions

(i) The water samples prepared with the same true color but with different apparent HS molecular sizes and different HA and FA percentages showed different coagulation behaviors. For water samples with the smallest apparent molecular size fractions, higher dosages of coagulant were needed (up to 432% higher), mainly because these water samples contained higher concentrations of FAs, which have a larger number of negatively charged groups.

(ii) It is recommended that the coagulation behaviors of waters from different sources never be extrapolated, even when such waters have similar true color values. It is necessary to conduct treatability studies to determine appropriate coagulation conditions and design parameters for each water type.

(iii) Coagulant dosage versus coagulation pH values were optimized and coagulation diagrams were constructed. Two distinct regions were observed in these diagrams in which coagulation, flocculation, and DAF using Fenton's reagent as a coagulant produced HS removal efficiencies $\geqslant 50$–60%. The first region occurred at a lower pH range (approximately 3.6–4.6) and required lower coagulant doses (Fenton). The second region occurred at a higher pH range (approximately 5.6–6.6) and required higher coagulant doses. In the first region, coagulation was dominated by the hydrolyzing species adsorption mechanism, resulting in charge neutralization of HS molecules. In the second region, $Fe(OH)_3$ precipitate formation was the likely removal mechanism, resulting in the adsorption of HS molecules and their incorporation into this precipitate. A restabilization region also appears to exist between the two regions of efficient coagulation.

(iv) With filtration experiments following DAF, the filtered water had remaining apparent color, turbidity, and total iron values of $\leqslant 3$ HU, 0.50 NTU (except for the last experiment, in which the value was $\leqslant 0.55$) and $0.005\,\mathrm{mg\,L^{-1}}$, respectively. These results comply with Brazilian and European drinking water standards (with respect to these parameters), and suggest that Fenton's reagent can be effectively used not only as an oxidant (as vastly applied in the literature) but also as a coagulant. Furthermore, the replacement of alum (one of the most widely used coagulants) by an iron salt (such as Fenton's reagent) may yield additional benefits because researchers have questioned the use of alum on the grounds that this product may cause health problems. It is therefore recommended that Fenton's reagent be added to the list of chemical products to be tested in treatability studies.

Acknowledgements

The authors are grateful to FAPESP (Fundação de Amparo à Pesquisa do Estado de São Paulo) for supporting this research (Process No. 02/04,622-1) and for providing the doctorate scholarships for the first (Process No. 02/07,680-2) and the fourth author (Process No. 00/0,786-5). The authors are also very grateful to Professor Eduardo Fausto de Almeida Neves (*in memorium*).

Symbols

CI — coagulation inefficient
DAF — dissolved air flotation
FA — fulvic acids
G_{fl} — flocculation average velocity gradient
G_{rm} — rapid-mix average velocity gradient
HA — humic acids
HS — humic substances
kDa — kilo Dalton
NOM — natural organic matter
T_{fl} — flocculation time
T_{rm} — rapid-mix time
TOC — total organic carbon
UF — ultrafiltration
UV_{254} — ultraviolet absorbance at 254 nm
V_f — flotation velocity
WTP — water treatment plant

References

[1] C. Richard, G. Guyot, J.-P. Aguer, A. Ter Halle, O.E. Trubetskaya, O.A. Trubetskoi, Role of fractionation in studying the photochemical properties of humic substances, Russ. J. Gen. Chem. 78(11) (2008) 2265–2272.

[2] F.J. Stevenson, Humus Chemistry: Genesis, Composition and Reactions, 2nd ed., Wiley, New York, NY, 1994.

[3] H.-C. Lin, G.-S. Wang, Effects of UV/H2O2 on NOM fractionation and corresponding DBPs formation, Desalination 270 (2011) 221–226.

[4] H. Selcuk, S. Meric, A.D. Nikolaou, M. Bekbolet, A comparative study on the control of disinfection by-products (DBPs) and toxicity in drinking water, Desalin. Water Treat. 26 (2011) 165–171.

[5] A.W. Zularisam, A.F. Ismail, R. Salim, Behaviours of natural organic matter in membrane filtration for surface water treatment—a review, Desalination 194 (2006) 211–231.

[6] L. Zheng, C. Huaqiang, D. Bingzhi, S. Fei, L. Hao, Pretreatment to enhance flux of ultrafiltration, Desalin. Water Treat. 30 (2011) 80–88.

[7] C.R. O'Melia, W.C. Becker, K-K. Au, Removal of humic substances by coagulation, J IAWQ, Water Sci. Technol. 40(9) (1999) 47–54.

[8] H. Katsumata, M. Sada, S. Kaneco, T. Suzuki, K. Ohta, Y. Yobiko, Humic acid degradation in aqueous solution by photo-Fenton process, Chem. Eng. J. 137 (2008) 225–230.

[9] S. Vreysen, A. Maes, Adsorption mechanism of humic and fulvic acid onto Mg/Al layered double hydroxides, Appl. Clay Sci. 38(3–4) (2008) 237–249.

[10] S. Hong, S. Kim, C. Bae, Efficiency of enhanced coagulation for removal of NOM and for adsorbability of NOM on GAC, Desalin. Water Treat. 2 (2009) 89–94.

[11] L. Fusheng, Y. Akira, A. Yuka, Characterization of micro-flocs of NOM coagulated by PACl, alum and polysilicate–iron in terms of molecular weight and floc size, Water Sci. Technol. 57(1) (2008) 83–90.

[12] G.R. Peyton, Understanding and optimizing ozone/UV treatment for the destruction of hazardous organic compounds in water: Mechanism efficiency and by-product, Detoxif. Hazard. Waste 1 (1988) 353–368.

[13] R.F.P. Nogueira, J.R. Guimarães, Photodegradation of dichloroacetic acid and 2,4-dichlorophenol by ferrioxalate/H_2O_2 system, Water Res. 34(3) (2000) 895–901.

[14] R. Fabris, C.W.K. Chow, M. Drikas, Practical application of a combined treatment process for removal of recalcitrant NOM—alum and PAC, Water Sci. Technol.: Water Supply 4 (4) (2004) 89–94.

[15] M. Fukushima, K. Tatsumi, S. Nagao, Degradation characteristics of humic acid during photo-Fenton processes, Environ. Sci. Technol. 35(18) (2001) 3683–3690.

[16] C.A. Murray, S.A. Parsons, Removal of NOM from drinking water: Fenton's and photo-Fenton's processes, Chemosphere 54 (2004) 1017–1023.

[17] C.A. Murray, S.A. Parsons, Advanced oxidation processes: Flowsheet options for bulk natural organic matter removal, Water Sci. Technol.: Water Supply 4(4) (2004) 113–119.

[18] H. Ratnaweera, E. Gjessing, E. Oug, Influence of physical–chemical characteristics of natural organic matter (NOM) on coagulation properties: An analysis of eight Norwegian water sources, J IAWQ, Water Sci. Technol. 40(9) (1999) 89–95.

[19] S.X. Campos, E.M. Vieira, E.R. Azevedo, T.J. Bonagamba, L. Di Bernardo, Color removal by coagulation, flocculation and sedimentation from water containing humic substances with different apparent molecular sizes, J. Water Supply: Res. Technol. Aqua 56(5) (2007) 327–333.

[20] M.B.O. Duarte, E.P.H. Santos, A.P. Duarte, Comparison between diafiltration and concentration operation modes for the determination of permeation coefficients of humic substances through ultrafiltration membranes, Anal. Chim. Acta 442 (2001) 155–164.

[21] J. Duan, J. Gregory, Coagulation by hydrolysing metal salts, Adv. Colloid Inferface Sci. 100(102) (2003) 475–502.

[22] G.A. Edwards, A. Amirtharajah, Removing color caused by humic acids, J. AWWA, Res. Technol. 77(3) (1985) 50–57.

[23] Brazil, Health Ministerial. Resolution n˚ 2914, December, 2011 (in Portuguese).

[24] World Health Organization, Guidelines for Drinking-water Quality, WHO, First addendum to third edition, Recommendations, vol. 1, 2006.

[25] US-EPA, National Primary Drinking Water Regulations, 2009.

[26] Council Directive, 83/EC on the quality of water intended for human consumption, Official J. Eur. Commun., 1988.

[27] D. An, J.-X. Song, W. Gao, G.-G. Chen, N.-Y. Gao, Molecular weight distribution for NOM in different drinking water treatment processes, Desalin. Water Treat. 5 (2009) 267–274.

[28] J.C. Rojasb, J. Péreza, G. Garralónc, F. Plazac, B. Morenoa, M. A. Gómeza, Humic acids removal by aerated spiral-wound ultrafiltration membrane combined with coagulation–hydraulic flocculation, Desalination 266 (2011) 128–133.

[29] J.K. Edzwald (Ed.), Water quality & treatment—A handbook on drinking water, sixth ed., American Water Works Association and McGraw-Hill, Denver, 2011.

[30] P.C. Singer (Ed.), Formation and control of disinfection by-products in drinking water, American Water Works Association and McGraw-Hill, Denver, 1999.